

## Direct numerical simulation of turbulent plane Couette flow

By Moon Joo Lee<sup>1</sup>

Turbulent plane Couette flow was numerically simulated at a Reynolds number ( $U_w h/\nu$ ) of 6000, where  $U_w$  is the relative wall speed and  $h$  is half the channel-height. Unlike in Poiseuille flow, where the mean shear rate changes its sign at the centerline, the sign of mean shear rate in plane Couette flow remains the same across the whole channel. This difference is expected to yield several differences between the two flows, especially in the core region. The most significant and dramatic difference observed in the present work was the existence of large-scale structures in the core region of the plane Couette flow. The large eddies are extremely long in the flow direction and fill the entire channel (i.e. their vertical extent is  $2h$ ). The large-scale structures have the largest contribution from the wavenumber  $(k_x h, k_z h) = (0, \pm 1.5)$ , corresponding to a wavelength  $\Lambda_z/h \simeq 4$ . The secondary motion associated with the  $k_x h = 0$  mode consists of the large-scale vortices. The large eddies contribute about 30% of turbulent kinetic energy.

### 1. Introduction

Plane Couette flow is a paradigm of shear flows because of its simple flow geometry and fundamental fluid-mechanical characteristics. A fully-developed plane Couette flow has a constant shear stress,  $\tau = \mu dU/dy - \rho \overline{uv}$  (equal to its value at the walls,  $\tau_w = \mu dU/dy|_w$ ), across the entire channel,  $-1 \leq y/h \leq 1$ , be it laminar or turbulent. This prominent property results directly from the zero mean pressure gradient in the flow as it is driven by shear generated at two plane, solid boundaries that are in rectilinear, parallel movement (at speed  $U_w$ ) relative to each other.

Another characteristic of structural interest of the flow is that both the mean vorticity (or mean shear rate,  $S = dU/dy$ ) and turbulent shear stress ( $-\rho \overline{uv}$ ) are symmetric about the center plane ( $y/h = 0$ ), yielding a finite production rate ( $-\rho S \overline{uv}$ ) of turbulent kinetic energy even in the core region (say,  $0.2-0.5 \leq y_\perp/h < 1$ , where  $y_\perp$  is the distance normal to a nearest boundary). As a consequence, the profiles of turbulence intensities ( $\overline{u^2}$ ,  $\overline{v^2}$ ,  $\overline{w^2}$ ) differ significantly among the three components (see El Telbany & Reynolds 1982), indicative of a high degree of anisotropy in the flow. We hypothesize that the structures of turbulence (both statistical and instantaneous) in the core region of plane Couette flow would be quite different from those of Poiseuille flow. This issue has not been addressed before. In the vicinity of the walls, say  $y_\perp/h \leq 0.1-0.2$ , however, structures of turbulence in the two flows are expected to be similar, since the near-wall dynamics of a turbulent shear flow is primarily controlled by a mechanism universally represented by the

<sup>1</sup> Permanent address: Pohang Institute of Science and Technology, Pohang, Korea

'law of the wall.' Identification and characterization of the possible new structures in turbulent plane Couette flow is one of the central questions addressed in this study. It is our goal to understand the mechanism by which the boundary shearing produces turbulence structures different from those generated in a pressure-driven flow.

Despite its apparent importance as a paradigm of shear flows, turbulent plane Couette flow has not been studied extensively. In most previous experiments (Reichardt 1956, 1959; Robertson 1959; Robertson & Johnson 1970; Leutheusser & Chu 1971; El Telbany & Reynolds 1980, 1981), the length of the shearing boundary realized by employing either a (flexible) moving belt or a fluid interface had to be made short ( $L_B/h = 10\text{--}80$ ) since it is prone to deform at high speeds (or at high Reynolds numbers). Because of the difficulties arising from the moving boundaries, only the profiles of mean velocity, turbulent intensities and turbulent shear stress were obtained in most experiments, and measurements of higher-order statistics, if any, were limited to the streamwise direction (Robertson & Johnson 1970; Aydin & Leutheusser 1979, 1989). Direct numerical simulation approach taken in this work is ideally suited to study structures of turbulence in plane Couette flow without having such problems.

In this paper, we report the existence of the large-scale eddies in the core region of plane Couette flow. Some details of the kinematical characteristics of the large-scale structures are presented. Both the instantaneous and statistical structures of turbulence in the flow are compared with those in plane Poiseuille flow. Implications for turbulence modeling are also discussed.

## 2. Numerical methods

The three-dimensional, time-dependent Navier–Stokes equations were solved numerically for plane Couette flow at a Reynolds number ( $Re = U_w h/\nu$ ) of 6000; the Reynolds number  $Re_\tau = U_\tau h/\nu$  based on the wall-shear velocity  $U_\tau = (\nu dU/dy|_w)^{1/2}$  is about 170. The particular choice of the Reynolds number was made in order to compare with the results of plane Poiseuille flow reported by Kim, Moin & Moser (1987,  $Re_\tau = 180$ ). The simulation reported in this paper was carried out by using a pseudo-spectral method with Fourier and Chebyshev polynomial expansions in the horizontal ( $x, z$ ) and vertical ( $y$ ) directions, respectively. The spectral expansion of the main computation reported here had  $128 \times 129 \times 192$  (3 170 304) modes in  $(x, y, z)$ . The computational domain has the streamwise and spanwise dimensions of  $(B_x, B_z)/h = (4\pi, \frac{8}{3}\pi)$ . No-slip and periodic boundary conditions were used at the walls and in the horizontal directions, respectively.

Time advancement was made through a low-storage, third-order Runge-Kutta method for the nonlinear terms and the second-order Crank–Nicolson scheme for the viscous terms. The initial field consisted of finite-amplitude random disturbances (about 10% of  $U_w$ ) in all components of velocity with the linear mean profile,  $U/U_w = \frac{1}{2}(y/h + 1)$ . Subsequent development of the basic statistics such as the mean velocity profile, turbulent kinetic energy and turbulent shear stress was monitored in order to determine whether the flow reached a statistical steady-state. The

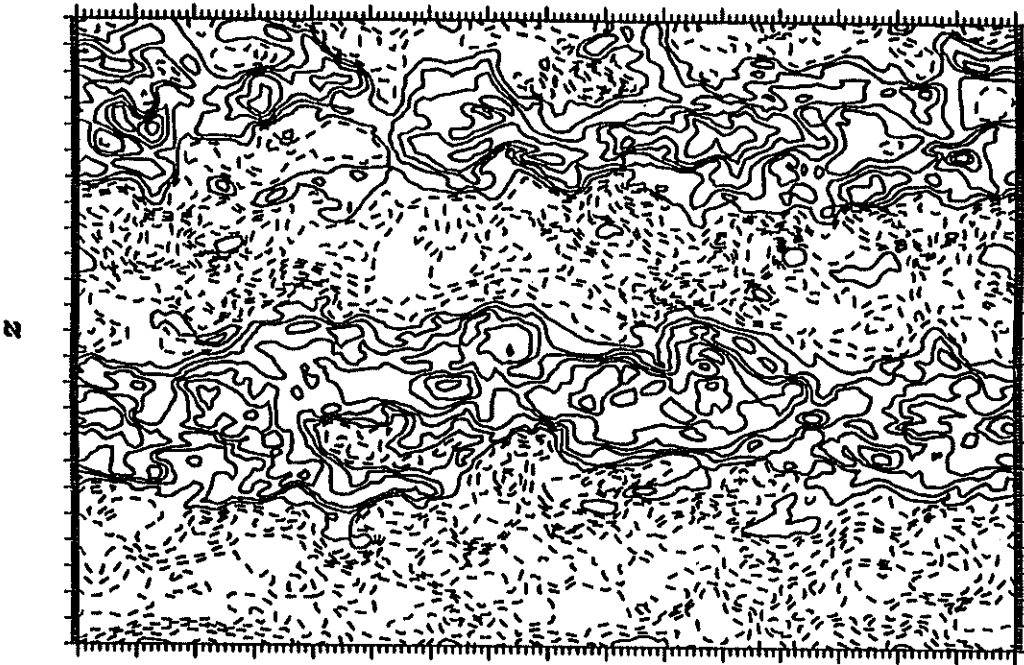
$x$ 

FIGURE 1. Contours of the instantaneous streamwise velocity ( $u$ ) at the center plane ( $y/h = 0$ ) of plane Couette flow: —,  $u \geq 0$ ; ----,  $u < 0$ .

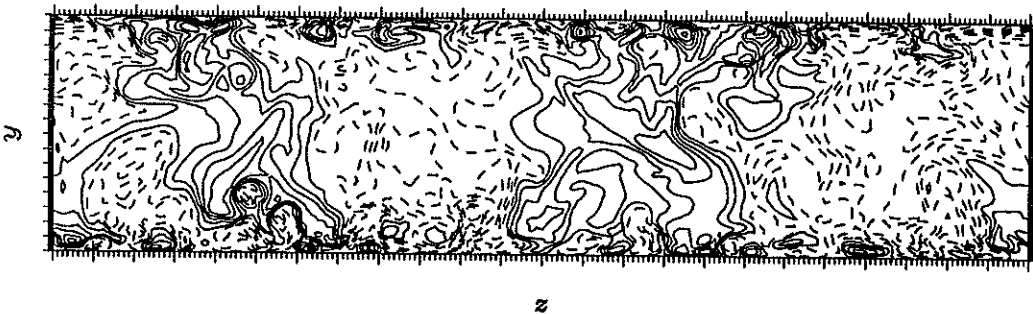


FIGURE 2. Contours of the instantaneous streamwise velocity ( $u$ ) on a  $yz$ -plane (an end view) of plane Couette flow: —,  $u \geq 0$ ; ----,  $u < 0$ .

computation was started with a coarse resolution ( $32 \times 65 \times 48$  modes), and when the flow reached a statistical steady-state, the number of modes was successively increased. The final statistics were compiled after the flow reached the statistical steady-state with the final resolution ( $128 \times 129 \times 192$  modes).

### 3. The large-scale structures

Contours of the instantaneous streamwise velocity ( $u$ ) at the center plane ( $y/h =$

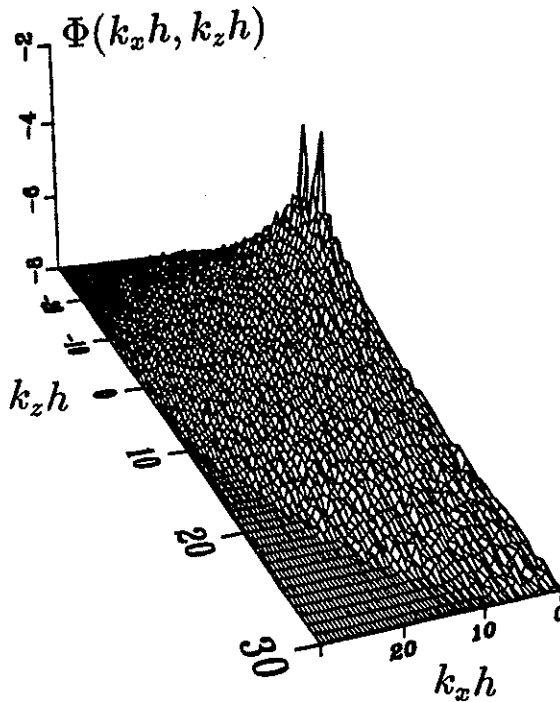


FIGURE 3. The two-dimensional energy spectrum  $\Phi(k_x h, k_z h) = \overline{|\hat{u}|^2}$  at the center plane ( $y/h = 0$ ) of plane Couette flow, showing that the energy density has two distinctive peaks at  $(k_x, k_z)h = (0, \pm 1.5)$ . The magnitude of the peaks is about seven times larger than the next largest contribution.

0) are shown in Figure 1. There are two pairs of high- and low-speed regions (denoted by solid and dashed lines in the figure) that are highly elongated in the flow direction and alternating in the spanwise direction. Note that the eddies are almost uniform in the flow direction (i.e. the eddies do not meander sideways much) and that the spanwise size of each region is about the channel-height ( $2h$ ). In plane Poiseuille flow where the mean shear rate changes sign at the center plane, there are no such organized structures of turbulence in the core region. The spanwise (one-dimensional) energy spectrum,  $\Theta_{uu}(k_z h)$ , of the streamwise velocity (not shown here) has a distinctive peak at  $k_z h = 1.5$ , which corresponds to a wavelength  $\Lambda_z/h \simeq 4$ , consistent with the instantaneous contours shown in Figure 1.

To examine the vertical extent of the eddy structures, contours of instantaneous  $u$  are drawn on a  $yz$ -plane (an end view) in Figure 2. The figure shows that the eddies are as tall as the whole channel height,  $2h$ , and hence the aspect ratio of the large eddies is close to unity. In the wall region, however, the presence of eddies of much smaller lengthscales is evident. These small wall-region eddies are identical to those found in the wall region of a plane Poiseuille flow.

The two-dimensional energy spectrum,  $\Phi(k_x h, k_z h) = \overline{|\hat{u}|^2}$ , at  $y/h = 0$  (Figure 3) shows that the energy density has two distinctive peaks at  $(k_x, k_z)h = (0, \pm 1.5)$ ;

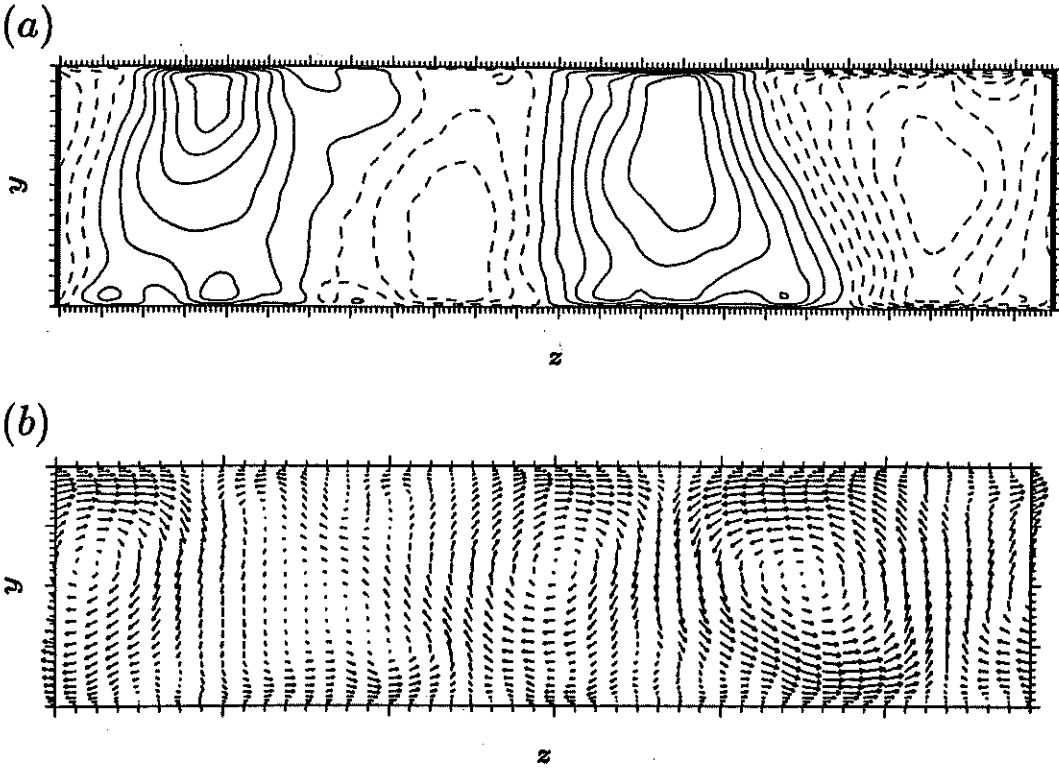


FIGURE 4. Velocity field of the  $k_x = 0$  mode (or the large-eddy field) in plane Couette flow. (a) Contours of  $\tilde{u}$  in the  $yz$ -plane (perpendicular to the mean flow); (b) velocity vectors,  $(\tilde{v}, \tilde{w})$ , projected on the  $yz$ -plane. —,  $\tilde{u} \geq 0$ ; ----,  $\tilde{u} < 0$ .

their magnitude is about seven times the next largest contribution. This dominant contribution of the  $(k_x, k_z)h = (0, \pm 1.5)$  mode persists even close to the walls (the ratio is about three at  $y_\perp/h = 0.001$ ), indicating that the large eddies have a significant effect across the whole channel.

To further investigate the characteristics associated with the large eddies, we decompose the flow field as  $\mathbf{v} = \tilde{\mathbf{v}} + \mathbf{v}'$ , where  $\tilde{\mathbf{v}} = (\tilde{u}, \tilde{v}, \tilde{w})$  is obtained by averaging over  $t$  and  $x$ , thus representing eddies independent of time and the streamwise direction (i.e., time-averaged  $k_x = 0$  mode), and  $\mathbf{v}'$  denotes the residual field. Contours of  $\tilde{u}$  in the  $yz$ -plane (perpendicular to the mean flow) are shown in Figure 4(a). The lengthscales associated with these large eddies are now more apparent; statistics associated with these eddies will be discussed in the next section. Note that the small-scale eddies that are quite strong in the instantaneous field (see Figure 2) are not present in the  $k_x = 0$  mode. In Figure 4(b), the velocity vectors,  $(\tilde{v}, \tilde{w})$ , projected on the  $yz$ -plane show that the secondary flow consists of large-scale vortices that fill the entire channel. (For visual clarity, every fourth data points in the both directions were selected for the vector plot.) Notice that in the core region the streamwise velocity ( $\tilde{u}$ ) is distributed  $180^\circ$  out of phase with the vertical velocity

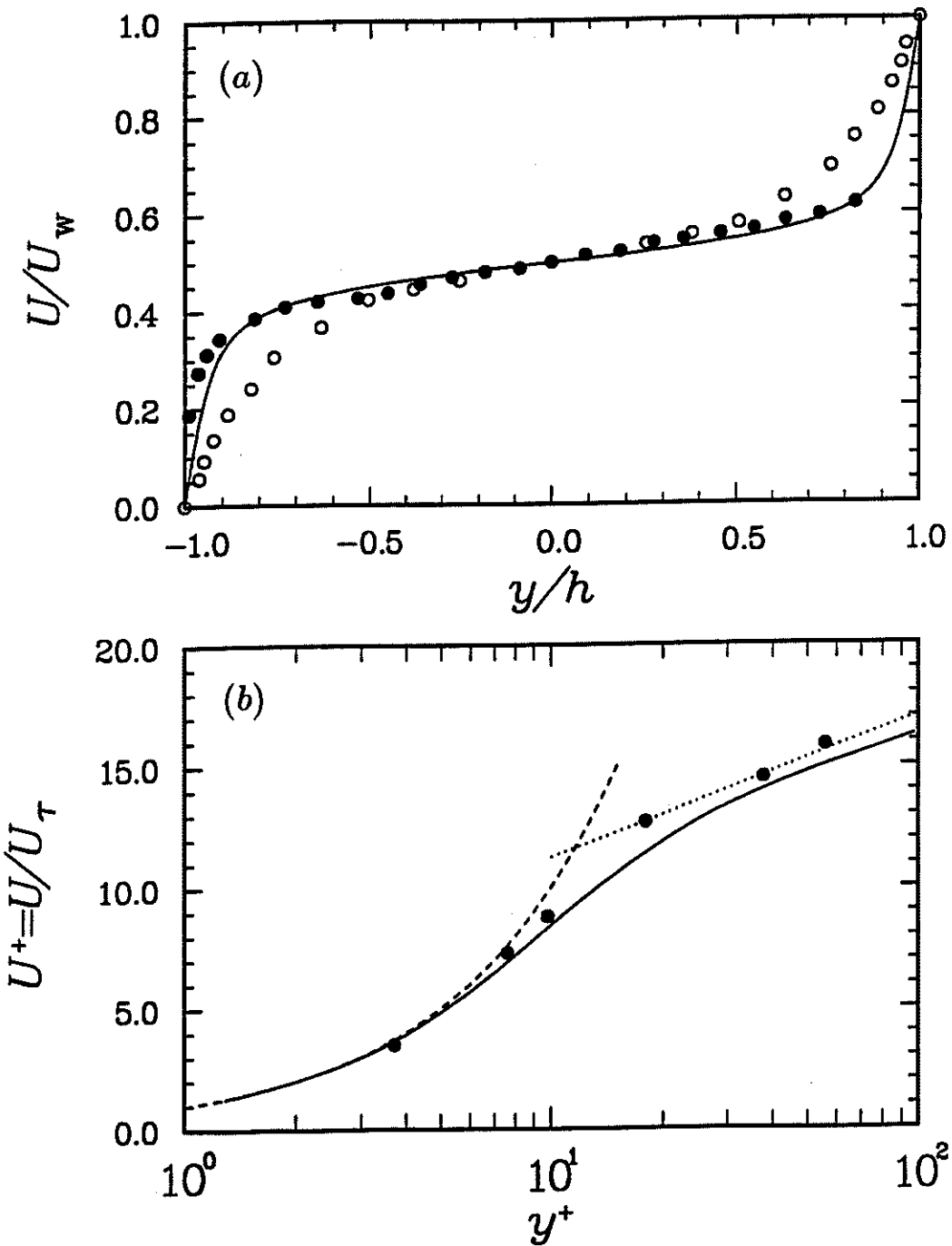


FIGURE 5. Mean velocity profile in plane Couette flow: (a) global profile,  $U/U_w$  vs.  $y/h$ ; (b) near-wall profile,  $U^+$  vs.  $y^+$ . —, present simulation; o, Reichardt (1959); •, El Telbany & Reynolds (1980); ----,  $U^+ = y^+$ ; ..... ,  $U^+ = (1/\kappa)\ln y^+ + B$  ( $\kappa = 0.4$  and  $B = 5.5$ ).

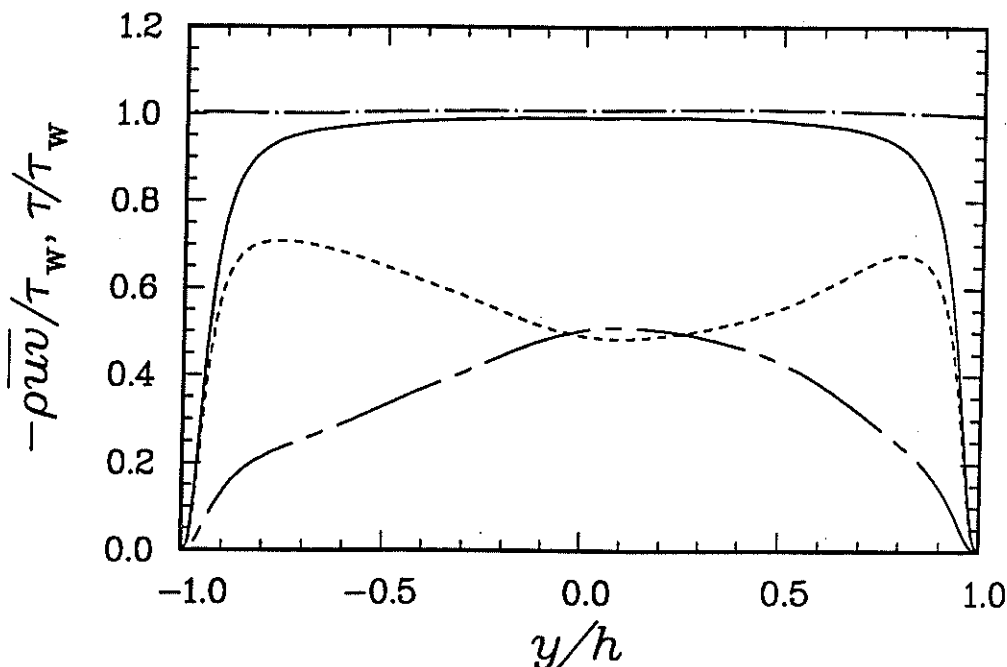


FIGURE 6. Profiles of shear stresses in plane Couette flow. —, total shear stress ( $\tau/\tau_w$ ); —, Reynolds stress ( $-\rho \overline{uv}$ ) of the full field; - - -, Reynolds stress of the  $k_x = 0$  mode; ····, Reynolds stress of the residual field.

( $\tilde{v}$ ), which leads to a significant contribution to shear stress from the secondary flow. Because of the large lengthscale of the secondary motion, the magnitude of its streamwise vorticity in the core region is only a few percent of the shear rate at the wall.

#### 4. Statistics

In Figure 5(a), comparison of the mean velocity profile,  $U$ , is made between the computation and experiments conducted at different Reynolds numbers ( $Re = 2900$ , Reichardt 1959;  $Re \simeq 2 \times 10^4 - 4 \times 10^4$ , El Telbany & Reynolds 1980). Note that the velocity profile at high Reynolds numbers changes rapidly within the narrow region close to the walls (say,  $y_{\perp}/h \leq 0.1$ ), and that it has a seemingly constant slope in the core region ( $|y/h| \leq 0.5$ ). The mean velocity gradient at the walls,  $S_w = dU/dy|_w$ , grows substantially with Reynolds number, whereas at the center plane the slope,  $S_c = dU/dy|_{y/h=0}$ , decreases with increasing Reynolds numbers. The value of  $S_c$  is about 5% of the wall value and it is about 30% of the value of a laminar flow with a linear velocity profile. Thus, the total shear stress in the turbulent case is about ten times higher compared with the laminar value. The near-wall profile,  $U^+$  (made dimensionless by the wall-shear velocity,  $U_{\tau}$ ), vs.  $y^+$  (the distance normal to the nearest wall scaled by the viscous length,  $\ell_v = \nu/U_{\tau}$ ) is shown in Figure 5(b). The dashed and dotted lines denote the law of the wall:  $U^+ = y^+$  and

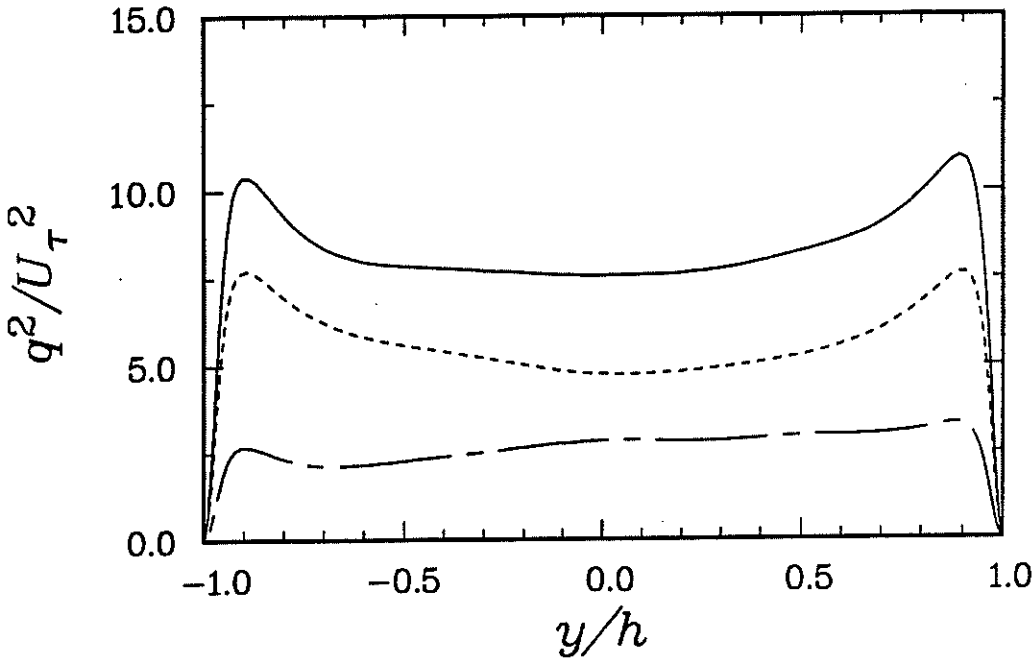


FIGURE 7. Profile of turbulent kinetic energy in plane Couette flow. —,  $q^2$  of the full field; ---,  $q^2$  of the  $k_x = 0$  mode; - · - ·,  $q^2$  of the residual field.

$U^+ = (1/\kappa) \ln y^+ + B$  (where  $\kappa = 0.4$  and  $B = 5.5$ ), respectively, which fits the experimental data at a higher Reynolds number (El Telbany & Reynolds 1980).

Figure 6 shows the profiles of turbulent and total shear stresses across the channel. The shear stresses are symmetric about  $y/h = 0$ , and the uniformity of the total shear stress ( $\tau/\tau_w = 1$ ) is apparent, indicating that the flow has indeed reached a statistical steady-state. Near the walls, the turbulent stress ( $-\rho \bar{u}v/\tau_w$ ) increases rapidly with the distance from the wall. (Hence, the mean shear rate,  $dU/dy = (\tau + \rho \bar{u}v)/\mu$ , decreases rapidly in the same vicinity of the walls.) In the core region, the total shear stress is completely dominated by the turbulent stress and the viscous stress is only a few percent.

It is of interest to examine how much the large-scale eddies contribute to energetics. In Figure 6, the contributions to the Reynolds stress from the large-scale eddies and residual field are drawn. The contribution from the large eddies increases with the distance from the wall and at the center line it is about the same as that from the residual field. Figure 7 compares the contributions to turbulent kinetic energy from the full, large-eddy and residual fields. Except in the vicinity of the wall (say  $y_{\perp}/h \leq 0.1$ ), the contribution from the large eddies is about 30% over the whole channel, indicative of the importance of the large-scale eddies.

The profiles of turbulence intensities ( $u'^+$ ,  $v'^+$ ,  $w'^+$ ) in Figure 8(a) show good agreement with the measurements (El Telbany & Reynolds 1981). Comparison with those in a plane Poiseuille flow (Figure 8b) at a comparable Reynolds number ( $Re_{\tau} =$



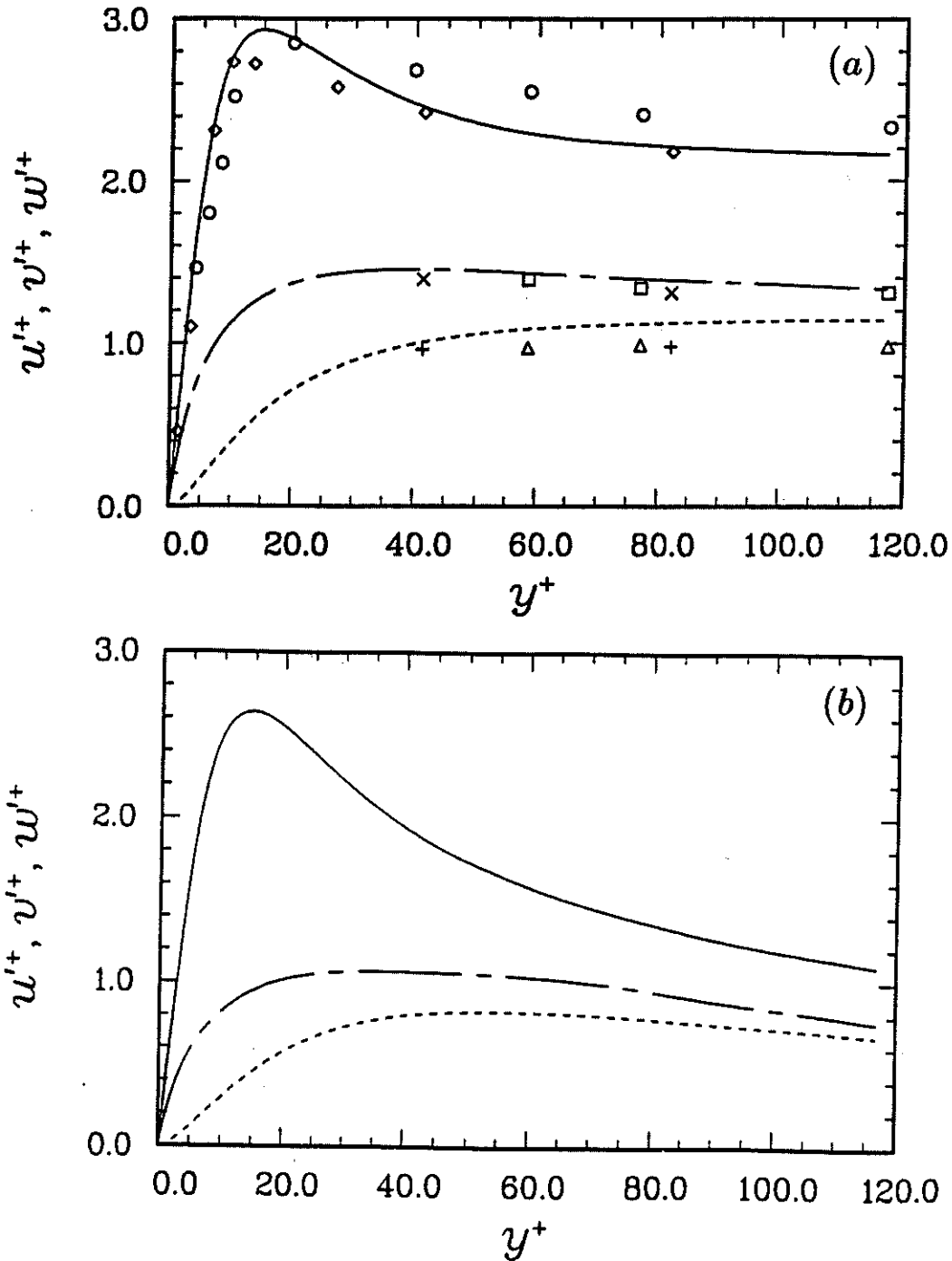


FIGURE 8. Near-wall profiles of turbulence intensities,  $(u'^+, v'^+, w'^+)$  vs.  $y^+$ : (a) plane Couette flow (present computation); (b) plane Poiseuille flow (from Kim *et al.* 1987). —,  $u'^+$ ; ----,  $v'^+$ ; ····,  $w'^+$ . Symbols are the measured data from El Telbany & Reynolds (1981).

180, Kim *et al.* 1987) shows that the intensities in Couette flow are significantly higher at most locations in the channel, except in the vicinity of the wall ( $y^+ \leq 30$ ) where the Couette values are only slightly higher. The marked difference in the core region is a direct consequence of the finite rate of production of turbulent kinetic energy in plane Couette flow. The figure also shows that the energy distribution among the three components in the core region is more anisotropic in Couette flow ( $\overline{u^2} : \overline{v^2} : \overline{w^2} \simeq 0.61 : 0.17 : 0.22$ ) than in Poiseuille flow.

## 5. Summary and concluding remarks

Direct numerical simulation of turbulent plane Couette flow at Reynolds number of 6000 was carried out. Examination of the instantaneous and statistical structures revealed the existence of large-scale eddies in the flow. The large-scale structures have an extremely long lengthscale in the flow direction and they fill the entire channel. They appear as pairs of high- and low-speed regions alternating in the spanwise direction with an average lengthscale of  $2h$  so that their aspect ratio is about unity. The  $(x, t)$ -averaged field shows the existence of secondary vortical motion that fills the entire channel.

It has been known that existing turbulence models based on two-dimensional flows have a difficulty in predicting structures of 'three-dimensional' flows such as curved channel flow and rotating channel flow. Despite the flow geometry of these flows is two-dimensional, large secondary flows develop and play a dominant role because of instabilities associated with centrifugal (curved channel) or Coriolis (rotating channel) force. Plane Couette flow does *not* have such instability, but similar large roll-cell-like structures exist in the core region as evidenced in the present work. Therefore, it would be of great interest to see how well the current turbulence models predict the behavior of turbulence in plane Couette flow.

We have also compiled a variety of turbulence statistics such as the probability density functions (and skewness and flatness) of velocity components, profiles of the terms in the transport equations of the Reynolds stresses, etc. Comparison with those in plane Poiseuille flow will be discussed in full later.

This work was performed in collaboration with John Kim of the NASA-Ames Research Center. I thank Parviz Moin and Javier Jimenez for the fruitful discussions. This work was supported in part by the National Science Foundation, for which I am grateful.

## REFERENCES

- AYDIN, M. & LEUTHEUSSER, H. J. 1979 Novel experimental facility for the study of plane Couette flow. *Rev. Sci. Instr.* **50**, 1362–1366.
- AYDIN, E. M. & LEUTHEUSSER, H. J. 1987 Experimental investigation of turbulent plane-Couette flow. *Forum on Turbulent Flows-1987*, FED vol. 51, 1987 ASME Applied Mech., Bioeng. & Fluids Eng. Conf., Cincinnati, Ohio, June 14–17, 1987 (ed. W. W. Bower), pp. 51–54. Amer. Soc. Mech. Eng.: New York.

- AYDIN, E. M. & LEUTHEUSSER, H. J. 1989 Plane-Couette flow between smooth and rough walls. *J. Fluid Mech. (sub judice)*
- EL TELBANY, M. M. M. & REYNOLDS, A. J. 1980 Velocity distributions in plane turbulent channel flows. *J. Fluid Mech.* **100**, 1-29.
- EL TELBANY, M. M. M. & REYNOLDS, A. J. 1981 Turbulence in plane channel flows. *J. Fluid Mech.* **111**, 283-318.
- EL TELBANY, M. M. M. & REYNOLDS, A. J. 1982 The structure of turbulent plane Couette flow. *Trans. ASME, J. Fluids Eng.* **104**, 367-372.
- KIM, J., MOIN, P. & MOSER, R. D. 1987 Turbulence statistics in fully developed channel flow at low Reynolds number. *J. Fluid Mech.* **177**, 133-166.
- LEE, M. J. 1990 The large-scale structures in turbulent plane Couette flow. *Center for Turbulence Research Annual Research Briefs-1989*, pp. 231-245. Center for Turbulence Research: Stanford University and NASA-Ames Research Center.
- LEUTHEUSSER, H. J. & CHU, V. H. 1971 Experiments on plane Couette flow. *Proc. ASCE, J. Hydr. Div.* **97** (HY9), 1269-1284.
- REICHARDT, H. 1956 Über die Geschwindigkeitsverteilung in einer geradlinigen turbulenten Couetteströmung. *Zeit. angew. Math. Mech.* **36**, Sonderheft 26-29.
- REICHARDT, H. 1959 Gesetzmäßigkeiten der geradlinigen turbulenten Couetteströmung. *Mitteil. Nr. 22*. Max-Planck-Inst. Strömungsforschung und Aerodynamischen Versuchsanstalt: Göttingen.
- ROBERTSON, J. M. 1959 On turbulent plane-Couette flow. *Proc. Sixth Midwestern Conf. Fluid Mech.*, Univ. of Texas, Austin, Texas, Sept. 9-11, 1959, pp. 169-182.
- ROBERTSON, J. M. & JOHNSON, H. F. 1970 Turbulence structure in plane Couette flow. *Proc. ASCE, J. Eng. Mech. Div.* **96** (EM6), 1171-1182.